Vol. 601: 97–108, 2018
https://doi.org/10.3354/meps12647

MARINE ECOLOGY PROGRESS SERIES
Mar Ecol Prog Ser

Published August 9

Oceanography and community structure drive zooplankton carbon and nitrogen dynamics in the eastern Bering Sea

Eric Hertz[1,5,*], M. Trudel[1,2,6], M. Carrasquilla-Henao[1], L. Eisner[3], E. V. Farley Jr.[4], J. H. Moss[4], J. M. Murphy[4], A. Mazumder[1]

[1]Department of Biology, University of Victoria, PO Box 3020, Station CSC, Victoria, BC V8W 3N5, Canada
[2]Pacific Biological Station, Fisheries and Oceans Canada, 3190 Hammond Bay Road, Nanaimo, BC V9T 6N7, Canada
[3]National Marine Fisheries Service, Alaska Fisheries Science Center, 7600 Sand Point Way NE, Bldg. 4, Seattle, WA 98115, USA
[4]National Marine Fisheries Service, Alaska Fisheries Science Center, Auke Bay Laboratories, Ted Stevens Marine Research Institute, 17109 Point Lena Loop Road, Juneau, AK 99801-8626, USA

[5]*Present address:* Pacific Salmon Foundation, #300-1682 West 7th Ave, Vancouver, BC V6J 4S6, Canada

[6]*Present address:* Fisheries and Oceans Canada, St. Andrews Biological Station, 531 Brandy Cove Road, St. Andrews, NB E5B 2L9, Canada

ABSTRACT: Bottom-up changes in the abundance and composition of primary producers and primary consumers can cascade through ecosystems. Zooplankton stable isotopes ($\delta^{13}C$ and $\delta^{15}N$) can be used to determine the linkages between these bottom-up processes, as nutrients, community composition, and physical oceanographic variables can influence zooplankton stable isotopes. However, the expression and variability in zooplankton stable isotopes remain poorly constrained and understood in many systems. Here, we explored how environmental and community variability influences zooplankton stable isotope ratios in the eastern Bering Sea across a wide range of ocean conditions. We tested whether there were interannual, spatial, or climate-driven shifts in the $\delta^{15}N$ and $\delta^{13}C$ of zooplankton. We found considerable variability across the eastern Bering Sea, with significant differences in isotopes among years, regions, and depths. These patterns were driven by differences in zooplankton community and physical oceanographic variables such as sea surface temperature. Effects were consistent across isotopes, and reflect the shared influences of oceanographic parameters and nutrients on $\delta^{13}C$ and $\delta^{15}N$ at the base of the food web.

KEY WORDS: Stable isotope · Isoscape · Chlorophyll *a* · Nitrate · Climate change

INTRODUCTION

There is great temporal and spatial variation in the abundance, distribution, and trophodynamics of organisms in marine environments. For lower trophic levels, the proximate cause of much of this variation may be local-scale processes in ocean conditions, but large-scale climate factors such as the North Pacific Gyre Oscillation or North Atlantic Oscillation can also contribute to differences in trophodynamics (Di Lorenzo et al. 2008, Mills et al. 2013, Hertz et al. 2016). Higher trophic level organisms can be influenced by these bottom-up processes, such that abundances of fish, seabirds, and marine mammals are affected by the abundance (Ware & Thomson 2005, Frank et al. 2006) and species composition (Trites & Donnelly 2003, Mackas et al. 2007, Mills et al. 2013) of lower tropic levels. Thus, understanding drivers of lower trophic level variation is important for understanding cascading changes throughout ecosystems.

The eastern Bering Sea is experiencing changes in ocean conditions due to climate change, and various aspects of the food web are responding in contrasting manners (Coyle et al. 2011). Zooplankton

*Corresponding author: ehertz@psf.ca

are a key prey item of many higher trophic level organisms, and represent a critical link in the eastern Bering Sea between primary producers and higher-order consumers (Coyle et al. 2011, Hunt et al. 2011). The abundance and species composition of zooplankton responds to shifts in climate conditions, with warmer years generally having zooplankton communities of a lower overall biomass comprised of smaller-sized individuals with lower lipid contents (Heintz et al. 2013, Eisner et al. 2014, Zador 2015). However, the implications of these shifts for higher trophic levels can be difficult to determine due to the different spatial and temporal scales on which they operate.

Because stable isotopes integrate variability in food chains over relatively longer time periods (weeks to months; Fry 2006), they are useful to understand the effects of shifting climatic conditions on marine food webs. In the ocean, $\delta^{15}N$ generally experiences an enrichment of 3–4‰ between trophic levels, and is thus often used as an indicator of trophic position (Cabana & Rasmussen 1996, Post 2002). However, biogeochemical and environmental factors can also alter $\delta^{15}N$ values at the level of dissolved inorganic nitrogen and subsequently phytoplankton, which is then passed on to higher trophic levels (McMahon et al. 2013, Schmittner & Somes 2016). The $\delta^{15}N$ of dissolved inorganic nitrogen, and thus the $\delta^{15}N$ of phytoplankton, is influenced by nutrient availability, nutrient source, light, species composition, and nitrogen fixation (Mullin et al. 1984, Somes et al. 2010, McMahon et al. 2013). On a global scale, water column denitrification, algal NO_3 uptake, and nitrogen fixation have the greatest impact on simulated $\delta^{15}N$, although local-scale effects can also override these broad-scale patterns (Somes et al. 2010).

$\delta^{13}C$ experiences a lower trophic enrichment, generally between 0 and 1‰, and is thus incorporated into consumer tissues relatively unmodified (Post 2002, McCutchan et al. 2003). Changes in phytoplankton $\delta^{13}C$ (and thus zooplankton $\delta^{13}C$) are generally caused by either changes in the $\delta^{13}C$ of dissolved inorganic carbon, or by differential fractionation during uptake and assimilation of dissolved inorganic carbon (Laws et al. 1995, Barnes et al. 2009). A positive relationship between sea surface temperature (SST) and phytoplankton $\delta^{13}C$ exists because the main parameters influencing photosynthetic fractionation of phytoplankton $\delta^{13}C$ are the concentration of dissolved CO_2 and the growth rate of the cells, both of which vary indirectly with SST (Laws et al. 1995, Magozzi et al. 2017). Lower temperatures and higher concentrations of CO_2 are associated with lower $\delta^{13}C$ values in phytoplankton (Rau et al. 1989, McMahon et al. 2013, Schmittner et al. 2013). Cell size, species composition, and growth rate are also all noted to influence phytoplankton $\delta^{13}C$ through differential fractionation (Laws et al. 1995, Popp et al. 1998), which can then be transferred up to higher-order consumers. Furthermore, when carbon drawdown is high during phytoplankton blooms, the nutrient source of phytoplankton can switch from dissolved CO_2 to bicarbonate ions, and due to differential fractionation between ions, phytoplankton experience enriched $\delta^{13}C$ values (Laws et al. 1997, Popp et al. 1998). Overall, in high-latitude systems, $\delta^{13}C$ of phytoplankton and zooplankton is expected to track SST gradients, as SST co-varies with direct drivers of phytoplankton isotopic fractionation such as community composition, growth rate, and concentration of dissolved CO_2 (Magozzi et al. 2017).

A growing number of studies in the ocean have generated large-scale isoscapes (McMahon et al. 2013, Magozzi et al. 2017) and have tested various hypotheses regarding large-scale baseline variability (Jennings & Warr 2003, Barnes et al. 2009). In the northeast Atlantic Ocean, baseline (queen scallop *Aequipecten opercularis*) spatial variability in $\delta^{13}C$ was largely controlled by temperature (Jennings & Warr 2003), while baseline spatial variability in $\delta^{15}N$ was related to temperature, as well as salinity and depth (Barnes et al. 2009). An isoscape developed with jellyfish tissue across the North Sea 10 yr later also showed similar patterns (MacKenzie et al. 2014). McMahon et al. (2013) synthesized isotopic data across the Atlantic Ocean and suggested the importance of changes in temperature, primary productivity, nutrients, microbial cycling, and phytoplankton composition and growth on baseline $\delta^{15}N$ and $\delta^{13}C$. Finally, Magozzi et al. (2017) used a coupled physics–biogeochemistry model to model the distribution of $\delta^{13}C$ of phytoplankton across the global ocean using modelled parameters such as SST, concentration of dissolved inorganic carbon, and concentration of CO_2.

A number of previous studies have investigated zooplankton stable isotopes in the eastern Bering Sea. Schell et al. (1998) and Schell (2000) hypothesized an annual positive relationship between chlorophyll *a* (chl *a*) concentrations (an indicator of phytoplankton biomass) and the $\delta^{13}C$ values occurring at the base of the food web in the Bering Sea. However, the relationship between environmental variables and stable isotopes of zooplankton was not directly assessed in these papers. Phytoplankton and zooplankton $\delta^{13}C$ could also be positively (though

indirectly) related to SST in the Bering Sea (Rau et al. 1989, Laws et al. 1995, Hertz et al. 2015). Patterns in zooplankton $\delta^{15}N$ in the eastern Bering Sea are less clear. Low $\delta^{15}N$ values were observed in the southern Bering Sea, possibly due to either slow phytoplankton growth rates or excess nutrient concentrations (Schell et al. 1998). Much of the variation in phytoplankton $\delta^{15}N$ in the Bering Sea could concern the source and composition of nitrogen used by phytoplankton (Somes et al. 2010), which correlates with nutrient concentrations and temperature. Omnivory within the zooplankton community may also be important for $\delta^{15}N$ values (Kling et al. 1992), with regions with more carnivorous zooplankton expected to have higher $\delta^{15}N$. Here, we add to this growing literature and show how commonly measured environmental variables influence $\delta^{13}C$ and $\delta^{15}N$ in zooplankton in the eastern Bering Sea.

Using stable isotopes as a tracer of bottom-up processes, we examined how environmental variability influences zooplankton stable isotopes in the eastern Bering Sea across variable temperature regimes. First, we tested whether there were interannual or spatial shifts in the $\delta^{15}N$ and $\delta^{13}C$ of zooplankton in the study period between 2003 and 2006. We expected significant differences in $\delta^{15}N$ and $\delta^{13}C$ due to variability in physical oceanography and nutrient concentrations, especially in 2006 when the eastern Bering Sea climate shifted from warmer to cooler conditions. We then examined whether predictions from global-scale models based on first principles matched with the variability observed across wide spatial scales in the eastern Bering Sea. We hypothesized that the $\delta^{13}C$ and $\delta^{15}N$ of zooplankton would be influenced by nutrients, SST, zooplankton community structure, and chl *a* (for $\delta^{13}C$), through the influence of these variables on dissolved inorganic nitrogen and carbon and subsequently phytoplankton. Finally, we modeled the spatial variation in the isotopic composition (isoscape) of nitrogen and carbon in the eastern Bering Sea over the period of 2003–2006.

MATERIALS AND METHODS

Survey stations and oceanographic sample collection

Bulk zooplankton samples and associated oceanographic data were collected in the eastern Bering Sea from August to early October 2003–2006 (n = 161, see Eisner et al. 2014 for more detailed sampling information). Stations were located from 54.4° to 64.0° N, and approximately 160° to 173° W (Fig. 1). Each station was sampled between 1 and 4 times (Fig. 1). Vertical profiles of temperature and chl *a* were collected using a Sea-Bird Electronics Model 25 or Model 9 plus CTD. Total integrated chl *a* (mg m^{-2}) at a given station was calculated by integrating the chl *a* concentrations over the water column estimated at 1 m intervals from CTD fluorometer profiles. The fluorometer was calibrated using discrete water samples for chl *a* collected with Niskin bottles attached to the CTD. Samples were filtered onto glass fiber filters, stored frozen at −80°C, and later analyzed with a bench top fluorometer using the acidification technique (Parsons et al. 1984). In 2003–2005, SST was recorded from the bridge using a thermosalinograph, while in 2006, SST

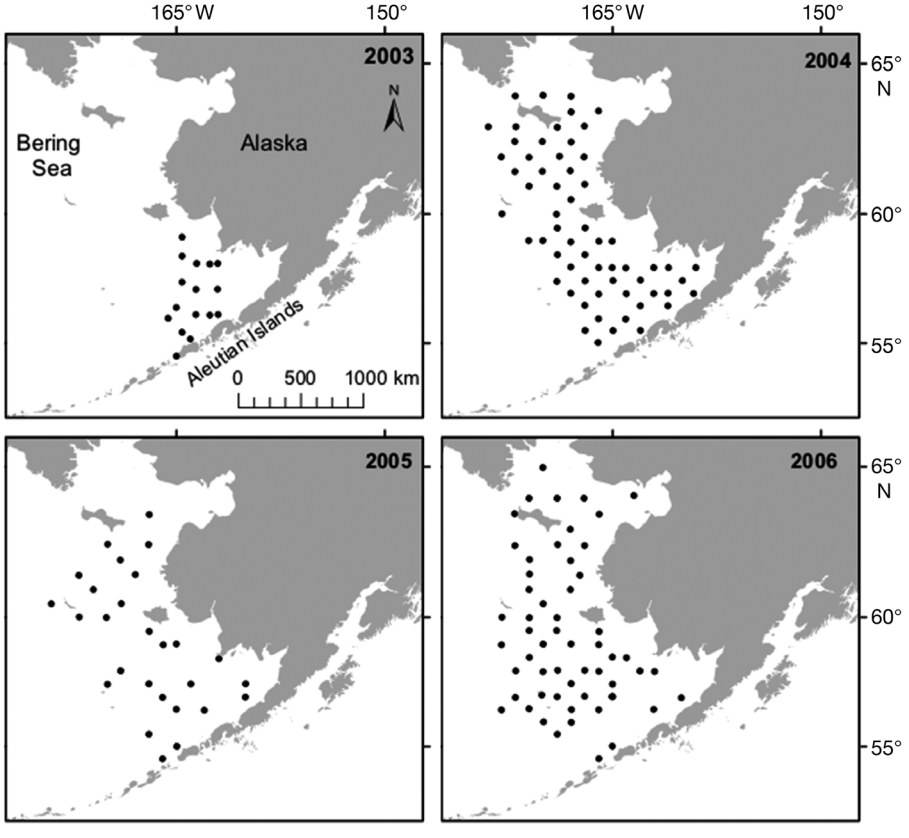

Fig. 1. Sampling stations in the Eastern Bering Sea, 2003–2006

data were recorded at 5 m from the CTD. These methods were not intercalibrated, but year was included as a random effect in all modeling (in part) to account for the possible variability. Water samples for nutrients were collected at 5 m using Niskin bottles on the CTD. Nutrient samples were frozen at −80°C and later analyzed for dissolved phosphate, silicic acid, nitrate, and nitrite at a shore-based facility using colorimetric methods (JGOFS 1994).

Bulk zooplankton for stable isotope analysis were collected with a 60 cm diameter bongo net with a 505 µm mesh towed obliquely from 5–10 m off bottom to the surface (or from 300 m to surface for bottom depths >300 m). Samples for stable isotope analysis were obtained using the entire catch from one side of the bongo, drained and stored frozen at −20°C. For taxonomy, samples from 2003 and 2004 were sorted at the Polish Plankton Sorting and Identification Center, while those from 2005 and 2006 were sorted at the University of Alaska (see Eisner et al. 2014 for more details). Samples for identification were stored in 5% buffered formalin.

Stable isotope analysis

Zooplankton samples were dried, ground to a fine powder, packed into tin capsules to approximately 1 mg, and run on a Thermo Delta IV Isotope Ratio Mass Spectrometer (University of Victoria). An internal standard showed measurement error of ~0.2‰. Values of $\delta^{15}N$ and $\delta^{13}C$ are expressed in the delta (δ) notation:

$$\delta^{15}N \text{ or } \delta^{13}C = [(R_{sample}/R_{standard}) - 1] \times 1000 \quad (1)$$

where R is ^{15}N:^{14}N or ^{13}C:^{12}C for the sample or a standard ($\delta^{15}N$ standard: atmospheric nitrogen; $\delta^{13}C$ standard: Vienna Peedee Belemnite). All samples of zooplankton were mathematically lipid-corrected using the C:N ratio following El-Sabaawi et al. (2009), since differences in the amount of lipids between samples can affect $\delta^{13}C$ values. C:N ratios of individual sample hauls ranged from 2.0 to 22.9, possibly due to differences in carbonate in the tissues among samples (Spero et al. 1997).

Statistical analysis

The statistical analysis had 3 separate goals. The first, descriptive, analysis explored whether the $\delta^{15}N$ and $\delta^{13}C$ of zooplankton was different among years (2003–2006), latitudinal regions (north: ≥60° N and south: <60° N), and cross-shelf depth domains (inner: <50 m, middle: 50–100 m, and outer: 100–180 m). However, the assumptions of parametric tests were not met in some comparisons and there was a negative relationship between the $\delta^{15}N$ and $\delta^{13}C$ of zooplankton ($R^2 = 0.28$, $p < 0.001$). We therefore used a permutation-based multivariate analysis of variance (PERMANOVA) to determine the effect of year, region, and depth domain (and their interactions) on $\delta^{15}N$ and $\delta^{13}C$ values. This analysis was carried out using the 'Adonis' function in the R package 'vegan' (Oksanen et al. 2018), using a Euclidean distance matrix (Coll et al. 2013). To further explore whether the categorical variables affected $\delta^{15}N$, $\delta^{13}C$, and C:N values differently, we also used separate Mann-Whitney *U*-tests and Kruskal-Wallis tests for $\delta^{15}N$ and $\delta^{13}C$. A post hoc test, 'kruskalmc', in the R package 'pgirmess' (Giraudoux 2018), was used to assess which groups were significantly different in the Kruskal-Wallis test.

The second analysis was concerned with determining how environmental, zooplankton community, and nutrient variables influenced zooplankton stable isotopes. To reduce the chances of spurious results, we carefully pre-selected possible variables for inclusion in the models (Burnham & Anderson 2002), based on mechanisms linking each variable to isotope variability, and on the availability of data sources. Environmental data included SST, surface (5 m) nitrate, silicate, and phosphate. For the $\delta^{13}C$ model, we also included water column integrated chl *a* biomass since chl *a* may have a positive (though indirect) correlation with phytoplankton $\delta^{13}C$. We included zooplankton community structure by running a principal component analysis (PCA) on the counts (m^{-3}) of the categories of species identified in the zooplankton tows. Categories that were represented in <5% of stations were removed for the purposes of this analysis (for categories retained, see Fig. S1 in the Supplement at www.int-res.com/articles/suppl/m601p097_supp.pdf). We used the scores from the first principal component as a predictor variable in the multi-model selection (Fig. S1).

We checked for correlations among predictor variables using Pearson correlations. To normalize nutrient data, we log transformed [log (x + 0.1)] all nutrient data prior to analysis (El-Sabaawi et al. 2012, 2013). To characterize associations between zooplankton isotopes ($\delta^{15}N$ and $\delta^{13}C$ separately) and environmental variables, we used regression and multimodel inference (Burnham & Anderson 2002). For model selection, we used Akaike's information criterion corrected for small sample sizes (AICc) and Akaike weight (w_i;

Burnham & Anderson 2002). As a rule of thumb, models with ΔAICc values within 2 of the best model are indistinguishable from the best model (Burnham & Anderson 2002). All explanatory variables were standardized to have a mean of 0 and standard deviation of 1 to allow interpretation of effect size and permit comparison of coefficients (Legendre & Legendre 1998). We accounted for spatial autocorrelation among variables by including an error structure where the association between sampling locations depended on a spherical distribution of latitude and longitude values (Crawley 2012). Year was included as a random effect in all models to account for the same station being sampled in multiple years. We also performed model averaging so that we did not have to rely solely on the best estimated model. Model averaging increases precision and reduces bias associated with only interpreting the best estimated model (Burnham & Anderson 2002). We used the 'MuMin' package in R to calculate parameter estimates with different combinations of model parameters (Bartoń 2013). We then used confidence intervals averaged over the model set by weight to assess the magnitude and directionality of the variables' effect on $\delta^{15}N$ and $\delta^{13}C$. All models were fit using the R package 'nlme' (Pinheiro et al. 2017).

The third goal was to create 'isoscapes' of spatial variability in $\delta^{15}N$ and $\delta^{13}C$ across the eastern Bering Sea. To do so, we used kriging interpolation, a geostatistical model used to interpolate measured values across a certain region. This method is more robust than alternative interpolation methods because it accounts for spatial autocorrelation in the model. We estimated the $\delta^{15}N$ and $\delta^{13}C$ across the eastern Bering Sea for all years combined (and each year separately) based on ordinary kriging and a spherical semivariogram model. We first estimated the semivariogram parameters (i.e. nugget, range, and sill) for each isotope in R and then included those values in the input of the kriging interpolation in ArcMap 10.3.1.

Table 1. Results of permutation-based multivariate analysis of variance (999 permutations) for the effects of year, region, and depth domain and interactions among variables on $\delta^{15}N$ and $\delta^{13}C$ of zooplankton. *denotes significant effects

	df	Mean	SumSq	*F*	R^2	p(>*F*)
Year	1	80.70	80.70	13.61	0.05	0.001*
Region	1	307.50	307.50	51.87	0.19	0.001*
Depth domain	2	219.85	109.92	18.54	0.14	0.001*
Year:Region	1	14.58	14.56	2.46	0.01	0.079
Year:Depth domain	2	48.50	24.25	4.09	0.03	0.008*
Region:Depth domain	1	19.92	19.92	3.36	0.01	0.053
Year:Region:Depth domain	1	9.08	9.08	1.53	0.01	0.211
Residuals	151	895.14	5.93		0.56	
Total	160	1595.26			1.00	

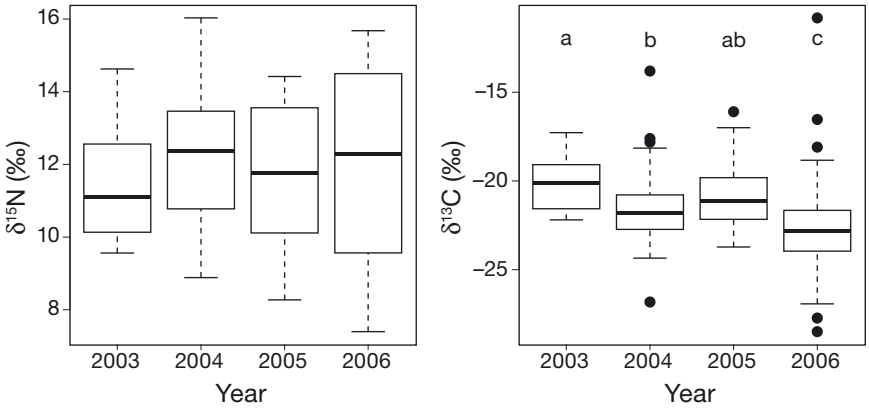

Fig. 2. Variability in $\delta^{15}N$ and $\delta^{13}C$ of Bering Sea bulk zooplankton by year. Different letters correspond to significant differences ($p < 0.05$) between years. Boxplots display the median and upper and lower quartiles, while whiskers display data within 1.5× the interquartile range from the box. Circles represent outliers

RESULTS

The PERMANOVA showed that year, region, and depth domain were all significant sources of variation of zooplankton $\delta^{15}N$ and $\delta^{13}C$ (Table 1). Interactions among these variables were only significant for year × depth domain (Table 1), suggesting that relationship between zooplankton $\delta^{15}N$ and $\delta^{13}C$ varied by year across the depth domains. To further partition variability, we also explored the effect of these categorical variables on zooplankton $\delta^{15}N$ and $\delta^{13}C$ separately.

Year

Over the 4 yr in this study, there were no significant differences between years for zooplankton $\delta^{15}N$ values (Kruskal-Wallis chi-squared = 3.4, df = 3, p = 0.33; Fig. 2). Zooplankton $\delta^{13}C$ values, on the other hand, showed significant interannual differences (Kruskal-Wallis chi-squared = 33.0, df = 3, $p < 0.0001$), although 2003 and 2005, and 2004 and 2005 were not significantly different (Fig. 2). There were no interannual differences in the

C:N ratio of zooplankton (Kruskal-Wallis chi-squared = 6.9, df = 3, p = 0.08).

Regional variability

There were no differences between the northern Bering Sea (60° N) and southern Bering Sea with respect to $\delta^{15}N$ (Wilcoxon rank sum test W = 2806, p = 0.58; Fig. 3). Similarly, the southern Bering Sea and the northern Bering Sea were not significantly different with respect to $\delta^{13}C$ (Wilcoxon rank sum test W = 1464, p = 0.46; Fig. 3). The southern Bering Sea did have a higher C:N ratio (Wilcoxon rank sum test W = 3891, p = 0.001).

Depth domain

All depth domains differed significantly in their $\delta^{15}N$ values (Kruskal-Wallis chi-squared = 60.5, df = 2, p < 0.0001), with values decreasing from near 13‰ in the middle domain to near 9‰ in the outer domain (Fig. 4). Depth domain also differed significantly for $\delta^{13}C$ (Kruskal-Wallis chi-squared = 34.1, df = 2, p < 0.0001), with the lowest values in the middle domain, but the comparison between the middle and outer domain was not significant (Fig. 4). C:N ratio also differed by depth domain (Kruskal-Wallis chi-squared = 21.6, df = 2, p < 0.0001) with the highest values near 10 in the outer domain, and non-significant differences near 6 for the inner and middle domains.

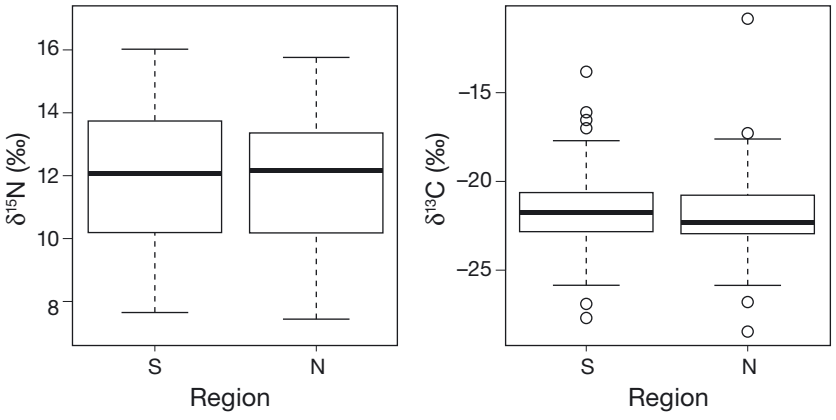

Fig. 3. Variability in $\delta^{15}N$ and $\delta^{13}C$ of Bering Sea bulk zooplankton by north (N) and south (S) region. See Fig. 2 for boxplot parameter definitions

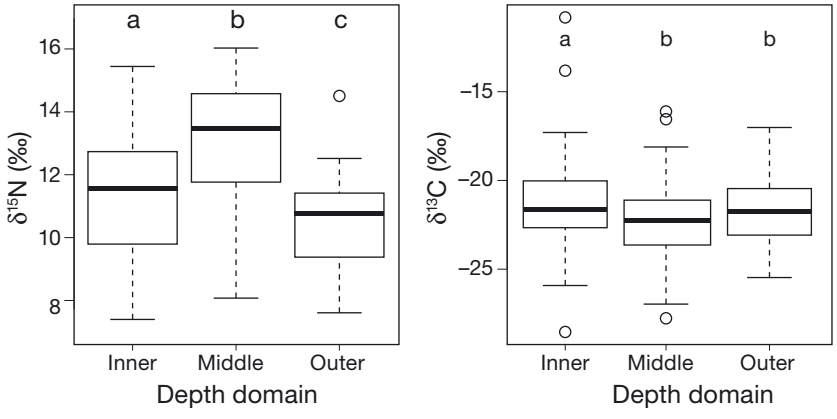

Fig. 4. Variability in $\delta^{15}N$ and $\delta^{13}C$ of Bering Sea bulk zooplankton by inner, middle, and outer depth domain. See Fig. 2 for boxplot parameter definitions

Environmental influences on zooplankton stable isotopes

Correlations between predictor variables were generally below r = 0.30, except for the correlations between nutrient concentrations. There was a significant positive Pearson's correlation between $\log(NO_3 + 0.1)$ and $\log(SiO_4 + 0.1)$ ($t_{159} = 11.2$, p < 0.001), between $\log(NO_3 + 0.1)$ and $\log(PO_4 + 0.1)$ ($t_{159} = 8.1$, p < 0.001), and between $\log(SiO_4 + 0.1)$ and $\log(PO_4 + 0.1)$ ($t_{159} = 8.6$, p < 0.001). Because of these strong correlations between nutrient values, we only used $\log(NO_3 + 0.1)$ as a predictor variable for the global model. The average SST recorded in this study was 12.2°C in 2003, 10.7°C in 2004, 10.6°C in 2005, and 9.0°C in 2006, similar to the anomalies calculated by Coyle et al. (2011). The average integrated chl *a* across the study area was 53.8 mg m^{-2} in 2003, 52.4 in 2004, 51.0 in 2005 and 65.7 in 2006, which is a slightly different pattern than reported in Eisner et al. (2016), likely due to sampling different stations in different years. Average surface NO_3 was 1.2, 0.73, 1.7, and 1.1 µM in 2003–2006, respectively.

Chaetognaths and amphipods, which feed at a higher trophic level than other zooplankton in the eastern Bering Sea (Schell et al. 1998), comprised a significant portion of the species composition at some stations (chaetognaths: 0–92%; amphipods 0–52%). There was a slight positive relationship between the % composition of chaetognaths at a station and $\delta^{15}N$ values (linear model: p = 0.02, R^2 = 0.03) and no relationship between the % composition of amphipods at a station and $\delta^{15}N$ values (linear model: p = 0.46,

Table 2. Confidence set of regression models for $\delta^{15}N$ of zooplankton in the Bering Sea from 2003 to 2006. Akaike's information criterion (AICc), AIC difference (Δ), and weight (w_i) are presented for the candidate models, which included all possible combinations of parameters plus the null model. The model set is presented in ascending order of Δ, which is the difference in AIC between the given model and the best-fitting model. $PC1_{Comm}$: scores from the first principal component of the zooplankton abundance matrix. SST: sea surface temperature. Dashes indicate parameters not included in the model

Intercept	$PC1_{Comm}$	NO_3	SST	AICc	Δ	w_i
11.96	0.74	–	−0.60	638.9	0.0	0.54
11.96	0.72	−0.19	−0.62	639.2	0.3	0.46
11.87	0.68	–	–	654.0	15.1	0.00
11.87	0.67	−0.13	–	655.4	16.5	0.00
11.95	–	−0.35	−0.38	702.7	63.8	0.00
11.95	–	–	−0.34	705.1	66.2	0.00
11.96	–	−0.30	–	705.4	66.5	0.00
11.96	–	–	–	706.7	67.8	0.00

R^2 = 0.00). Both of these categories were included in the principal component analysis (with the other species categories) to determine loadings of overall species composition, and influence of species composition on $\delta^{15}N$ and $\delta^{13}C$ values.

The first principal component of the zooplankton abundance matrix explained 15.4% of the variation (Fig. S1; hereafter $PC1_{Comm}$). *Epilabidocera amphitrites*, Caridea spp., and Gammaridae spp. loaded strongly positive on PC1, while *Metridia pacifica*, *Neocalanus* spp., and Hyperiidae spp. loaded strongly negative on PC1 (see Table S1 in the Supplement). The scores from this principal component from each station were used as an explanatory variable in the spatial models.

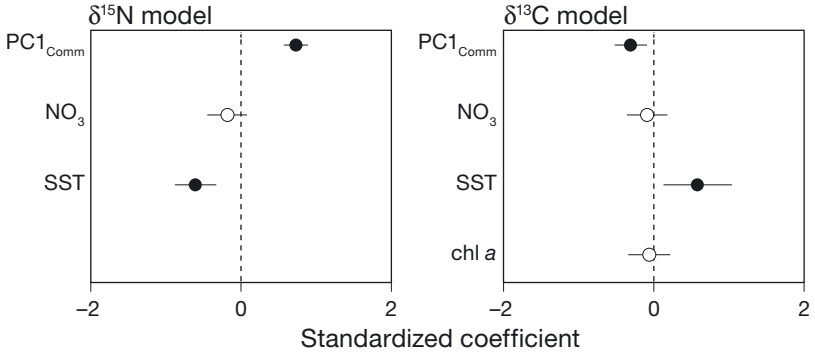

Fig. 5. Model averaged parameter coefficients (with 95% confidence limits) for zooplankton $\delta^{15}N$ and $\delta^{13}C$ in the eastern Bering Sea. Values are significant ($p < 0.05$) if confidence intervals do not overlap with 0 (vertical dashed line) and are represented with a filled circle. Non-significant variables are represented by an open circle. $PC1_{Comm}$: scores from the first principal component of the zooplankton abundance matrix, SST: sea surface temperature

Table 3. As in Table 2, but for $\delta^{13}C$

Intercept	$PC1_{Comm}$	NO_3	SST	chl *a*	AICc	Δ	w_i
−21.67	−0.31	–	0.59	–	670.2	0.0	0.56
−21.65	−0.32	−0.10	0.57	–	671.9	1.7	0.23
−21.52	−0.28	–	–	–	673.8	3.7	0.09
−21.65	−0.31	−0.09	0.57	−0.06	673.9	3.8	0.08
−21.52	−0.28	–	–	−0.06	675.8	5.7	0.03
−21.55	–	–	–	−0.09	680.0	9.8	0.00
−21.52	−0.38	–	0.55	−0.34	710.3	40.2	0.00
−21.37	−0.39	−0.28	–	−0.30	714.6	44.5	0.00
−21.35	−0.42	−0.32	–	–	715.6	45.4	0.00
−21.58	–	–	0.50	−0.45	721.9	51.7	0.00
−21.57	–	−0.12	0.48	−0.43	723.6	53.5	0.00
−21.43	–	−0.17	–	−0.42	726.1	56.0	0.00
−21.54	–	–	0.49	–	726.3	56.1	0.00
−21.53	–	−0.17	0.46	–	727.5	57.3	0.00
−21.40	–	–	–	–	729.1	59.0	0.00
−21.40	–	−0.22	–	–	729.7	59.5	0.00

The AIC model ranking indicated that given the set of candidate models for $\delta^{15}N$, the regression model that best described the variation included $PC1_{Comm}$ and SST, with a w_i of 0.54 (Table 2). The model that also included NO_3 had equivalent support (w_i = 0.46, delta = 0.3). The model averaged parameter values provided insight on the directionality and strength on the association of predictor variables with zooplankton $\delta^{15}N$ values. The zooplankton community structure had a strong positive effect on zooplankton $\delta^{15}N$ while SST had a strong negative effect (Fig. 5). The coefficient estimate for NO_3 overlapped 0.

The models that best explained the variation for $\delta^{13}C$ included the same parameters. The AIC model ranking for $\delta^{13}C$ indicated that the best model included $PC1_{Comm}$ and SST with a w_i of 0.56 (Table 3). The second-ranked model had a delta of 1.7, and included NO_3 in addition to $PC1_{Comm}$ and SST (w_i = 0.23). Model averaged parameter values for $\delta^{13}C$ showed a negative effect of zooplankton community structure and a positive but variable effect of SST (Fig. 5). The model averaged coefficient estimate for both NO_3 and chl *a* overlapped zero.

For both $\delta^{13}C$ and $\delta^{15}N$ models, the random effect of year explained less than 1% of the variance.

Isoscapes

The zooplankton $\delta^{15}N$ model parameters were a range of 601 km, a sill of 4.10,

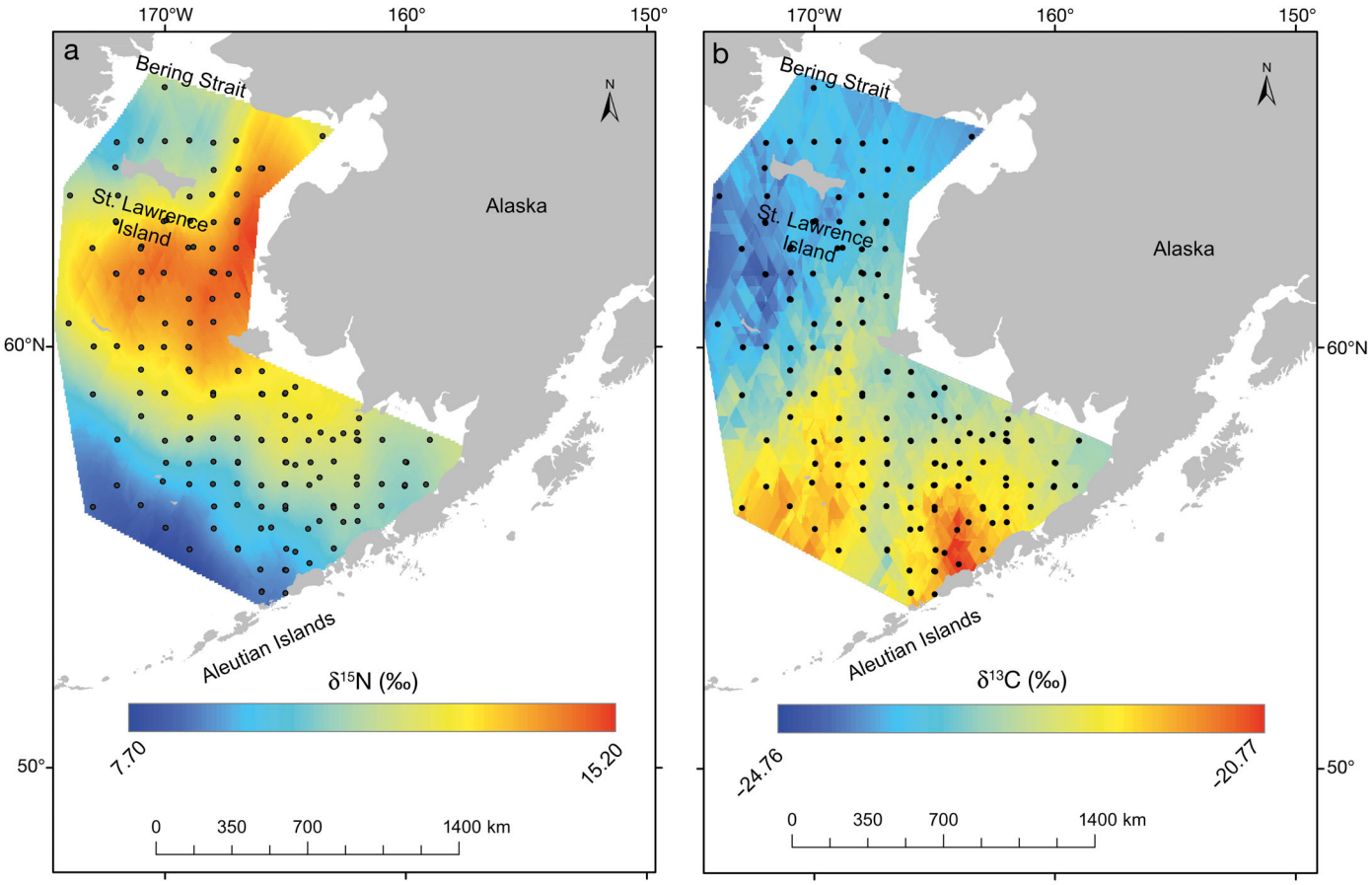

Fig. 6. (a) $\delta^{15}N$ and (b) $\delta^{13}C$ isoscape of the Eastern Bering Sea, 2003–2006. Black dots indicate all stations sampled between 2003 and 2006

and a nugget variance of 1.3. Across all years, zooplankton $\delta^{15}N$ was enriched in northern and eastern areas of the Bering Sea shelf, with values near 15‰ (Fig. 6a). In the Bering Strait, values were slightly lower, and there were depleted values of zooplankton $\delta^{15}N$ north and west of St. Lawrence Island. Towards the southeast of our sampling area, zooplankton $\delta^{15}N$ values were lower, and the lowest $\delta^{15}N$ values were in the southeast, with values near 8‰.

The zooplankton $\delta^{13}C$ model parameters showed a range of 1324 km, a sill of 2.03, and a nugget variance of 3.8. Zooplankton $\delta^{13}C$, across all years, showed an opposite pattern. Values were more depleted (lower) on the northern and eastern Bering Sea shelf, with a slight enrichment (rather than depletion as in $\delta^{15}N$) of values immediately north and east of St. Lawrence Island (Fig. 6b). The most enriched (highest) $\delta^{13}C$ values were in the south, near the Aleutian Islands. Both $\delta^{15}N$ and $\delta^{13}C$ showed the same general patterns when the data were split by year, although with some local-scale differences and changes in magnitude (Figs. S2 & S3 in the Supplement).

DISCUSSION

We found spatial and temporal variability in zooplankton carbon and nitrogen stable isotopes in the eastern Bering Sea. This variability appeared to be largely driven by differences in zooplankton community structure as well as physical oceanographic variables, such as SST. The effects were generally similar for both $\delta^{13}C$ and $\delta^{15}N$, and reflect shared processes driving carbon and nitrogen dynamics at the base of the foodweb. The spatial and temporal coverage of this study is notable, and data on the baseline variability in isotope dynamics within a critical region supporting major fisheries could prove useful for studies on isotopic variation in other species.

We found interannual differences in $\delta^{13}C$. This was especially evident in 2006, when the climate shifted from a warmer to a cooler regime (Coyle et al. 2011). This shift in climate was accompanied by a change in $\delta^{13}C$ values to the lowest observed over the 4 yr of our study. Both the spatial and temporal variations in $\delta^{13}C$ in the eastern Bering Sea are likely related to

SST, because with cooler SST, the amount of dissolved CO_2 increases, resulting in phytoplankton with lower $\delta^{13}C$ due to differential fractionation of CO_2 and bicarbonate ions (Weiss 1974, Laws et al. 1997, McMahon et al. 2013). Phytoplankton (and thus possibly zooplankton) isotopic fractionation is also influenced by SST through the indirect impact of SST on phytoplankton growth rate and cell size (Laws et al. 1995, Popp et al. 1998). Supporting the importance of SST in the eastern Bering Sea, the model-averaged parameter estimate for SST was large and positive, as expected.

Nutrients showed a limited effect on zooplankton $\delta^{13}C$. Nitrate (which was strongly and positively correlated to other nutrient concentrations) was also included in the second-best model for the spatial variation in $\delta^{13}C$. This may indicate the importance of nutrients on phytoplankton growth — if NO_3 was a limiting nutrient (Laws et al. 1997, McMahon et al. 2013) (e.g. higher nutrients lead to increases in phytoplankton growth and subsequent increases in zooplankton $\delta^{13}C$ that prey on the $\delta^{13}C$ enriched phytoplankton).

The effect of phytoplankton biomass (chl *a*) on $\delta^{13}C$ was relatively weak, with the model that included this extra parameter receiving much less AIC support compared to other models. This is likely because SST and nutrient concentrations may co-vary indirectly with chl *a*, but once both of these factors are included in the model, there is little additional variance that can be explained by chl *a*. Chl *a* offers a rough estimate of phytoplankton biomass rather than productivity (Schell et al. 1998, Miller et al. 2008, Oczkowski et al. 2014). Thus, the ship-board estimates of chl *a* biomass are only a snapshot in time reflecting the balance between growth and loss rates of phytoplankton that are temporally disconnected from the $\delta^{13}C$ of zooplankton (Woodland et al. 2012).

For $\delta^{13}C$, we also found that the community structure of zooplankton was an important factor in explaining spatial variation. Previous work on zooplankton in the Bering Sea has shown that the community structure varies both spatially and temporally, with general separation among taxonomic community clusters by both latitude and longitude (Eisner et al. 2014). Since we were analyzing bulk zooplankton, and we found that the zooplankton community structure was important for explaining variation in $\delta^{13}C$ (and $\delta^{15}N$), it is likely that zooplankton communities from different geographic regions were playing different trophic roles (Kling et al. 1992, El-Sabaawi et al. 2012). For example, the nearshore community (Cluster L1 in Eisner et al. 2014) was characterized by high abundances of *Parasagitta elegans* and Cnidaria, and this corresponds with relatively high values of $\delta^{13}C$ and $\delta^{15}N$ in our isoscapes. Both *P. elegans* and Cnidaria feed largely on other zooplankton, so would be expected to have higher isotope values as well. Further research could use a single zooplankton species to minimize variation in isoscapes caused by shifts in community composition (Kline 2010) or it could use compound-specific stable isotope analysis (Popp et al. 2007).

The same parameters that explained variability in $\delta^{13}C$ values also explained variability in $\delta^{15}N$ values. Because of the correlation between $\delta^{13}C$ and $\delta^{15}N$ ($R^2 = 0.28$, $p < 0.001$), it was difficult to partition out the factors driving each isotope independently. The only model-averaged parameters for $\delta^{15}N$ that did not overlap 0 included a negative estimate for SST, and a stronger positive estimate for $PC1_{Comm}$. In the California Current System, the $\delta^{15}N$ of zooplankton was strongly related to SST, possibly due to temperature effects on nitrate supply and demand (El-Sabaawi et al. 2012, 2013).

The isoscapes represent spatial and temporal variability in both $\delta^{13}C$ and $\delta^{15}N$. Spatially, $\delta^{15}N$ values tended to be highest in the northern Bering Sea, and in nearshore areas. These regional differences in stable isotopes were also indicated by the significance of the depth domain variable in the PERMANOVA. Overall, with the data from 2003–2006 combined in an isoscape, the Bering Strait was relatively enriched in $\delta^{15}N$ relative to regions just south (north of St. Lawrence Island). In isoscapes developed from data in 2004 and 2006, despite limited sampling in the region, it appeared that the Bering Strait had lower $\delta^{15}N$ values than more nearshore or southern areas. This could be due to interannual differences in the advection of zooplankton from the nutrient-rich Anadyr water through the Bering Strait and into the Chukchi Sea (Schell et al. 1998, Marsh et al. 2016), or simply interannual variability in NO_3. The increase of $\delta^{15}N$ from offshore to nearshore areas of the eastern Bering Sea indicates the low surface concentrations of nitrate (Schell et al. 1998; our Fig. 7). Contrastingly, in the south Bering Sea (near the Aleutian Islands), Schell et al. (1998) suggested that the very depleted $\delta^{15}N$ values were due to slow phytoplankton growth rates or excess nutrient concentrations. We found that the surface nitrate concentrations were very high in the south of the Bering Sea relative to the rest of the Bering Sea (Fig. 7), lending support to the excess nutrient concentration hypothesis.

$\delta^{13}C$ values in the eastern Bering Sea were enriched in the south (near the Aleutian Islands) com-

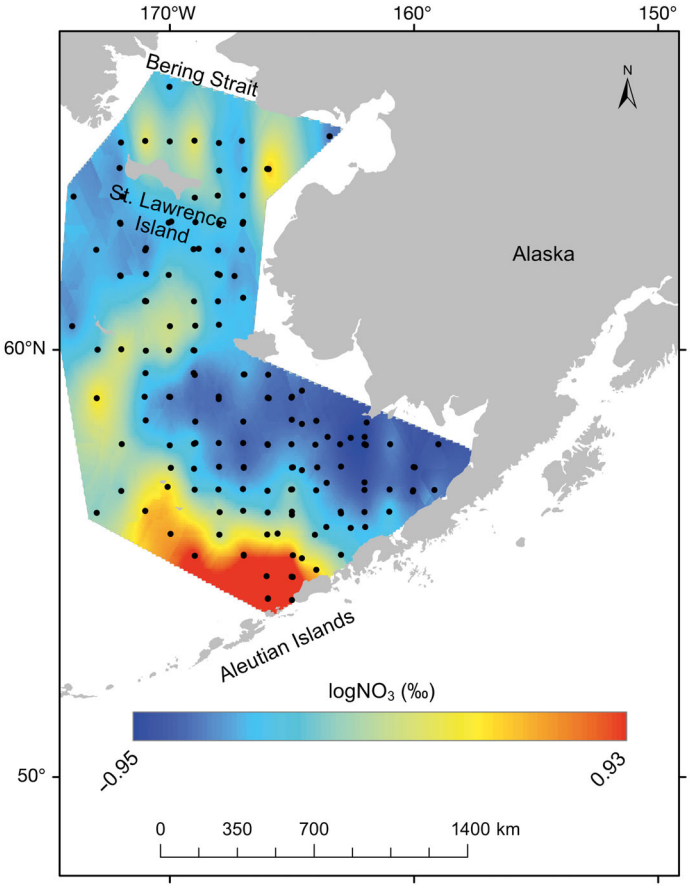

Fig. 7. Nitrate [log (x + 0.1)] at the surface (5 m) in the eastern Bering Sea, 2003–2006. Black dots indicate all stations sampled between 2003 and 2006

pared to more northern regions. Part of this pattern could be due to the northern Bering Sea having lower SST (Eisner et al. 2016), leading to higher concentrations of CO_2, and associated depleted $\delta^{13}C$ due to preferential use of the light isotope by phytoplankton when concentrations are higher (Laws et al. 1995, Hertz et al. 2015, Magozzi et al. 2017).

Estimating trophic relationships between organisms using bulk zooplankton requires that the baseline variability in isotopes is known (Cabana & Rasmussen 1996, Jennings & Warr 2003, Warry et al. 2016). We have shown that the baseline variability in both $\delta^{15}N$ and $\delta^{13}C$ can be high on large spatial scales, and can be driven by physical oceanographic variables, zooplankton community structure, and nutrient availability. Future research could use the isoscapes and models that we have developed here for the eastern Bering Sea to better understand processes occurring at higher trophic levels, especially given the projected changes in temperature and ice cover in the Bering Sea because of increased greenhouse gas emissions and climate forcing. These data could also be quantitatively compared to global-scale mechanistic models (Somes et al. 2010, Magozzi et al. 2017), to determine how well predictions made in the eastern Bering Sea match up with observed patterns.

Acknowledgements. We thank the captains and crews of the charter fishing vessels 'Sea Storm' and 'NW Explorer' for carrying out field sampling. We thank NOAA scientific staff and volunteers for assistance with sampling, processing, and database management. Thanks to the anonymous reviewers for constructive feedback on the manuscript and to Jillian Dunic and Geoff Osgood for statistical direction and advice. This project was supported by an NSERC Discovery Grant to A.M.

LITERATURE CITED

Barnes C, Jennings S, Barry JT (2009) Environmental correlates of large-scale spatial variation in the $\delta^{13}C$ of marine animals. Estuar Coast Shelf Sci 81:368–374

Bartoń K (2013) MuMIn: multi-model inference. R package version 1.9.13. The Comprehensive R Archive Network (CRAN), Vienna. https://cran-r.project.org/web/packages/MuMin/index.html

Burnham KP, Anderson DR (2002) Model selection and multimodel inference: a practical information-theoretic approach, 2nd edn. Springer Science & Business Media, New York, NY

Cabana G, Rasmussen JB (1996) Comparison of aquatic food chains using nitrogen isotopes. Proc Natl Acad Sci USA 93:10844–10847

Coll M, Navarro J, Olson RJ, Christensen V (2013) Assessing the trophic position and ecological role of squids in marine ecosystems by means of food-web models. Deep Sea Res II 95:21–36

Coyle KO, Eisner LB, Mueter FJ, Pinchuk AI and others (2011) Climate change in the southeastern Bering Sea: impacts on pollock stocks and implications for the oscillating control hypothesis. Fish Oceanogr 20:139–156

Crawley MJ (2012) The R book. John Wiley & Sons, Mississauga

Di Lorenzo E, Schneider N, Cobb KM, Franks PJS and others (2008) North Pacific Gyre Oscillation links ocean climate and ecosystem change. Geophys Res Lett 35: L08607

Eisner LB, Napp JM, Mier KL, Pinchuk AI, Andrews AG III (2014) Climate-mediated changes in zooplankton community structure for the eastern Bering Sea. Deep Sea Res II 109:157–171

Eisner LB, Gann JC, Ladd C, Cieciel KD, Mordy CW (2016) Late summer/early fall phytoplankton biomass (chlorophyll *a*) in the eastern Bering Sea: spatial and temporal variations and factors affecting chlorophyll *a* concentrations. Deep Sea Res II 134:100–114

El-Sabaawi R, Dower JF, Kainz M, Mazumder A (2009) Characterizing dietary variability and trophic positions of coastal calanoid copepods: insight from stable isotopes and fatty acids. Mar Biol 156:225–237

El-Sabaawi R, Trudel M, Mackas DL, Dower JF, Mazumder A (2012) Interannual variability in bottom-up processes in the upstream range of the California Current system: an isotopic approach. Prog Oceanogr 106:16–27

El-Sabaawi R, Trudel M, Mazumder A (2013) Zooplankton stable isotopes as integrators of bottom-up variability in coastal margins: a case study from the Strait of Georgia and adjacent coastal regions. Prog Oceanogr 115:76–89

Frank KT, Petrie B, Shackell NL, Choi JS (2006) Reconciling differences in trophic control in mid latitude marine ecosystems. Ecol Lett 9:1096–1105

Fry B (2006) Stable isotope ecology. Springer Science & Business Media, New York, NY

Giraudoux P (2018) Package 'pgirmess': data analysis in ecology. http://cran.r-project.org/web/packages/pgirmess/pgirmess.pdf

Heintz RA, Siddon EC, Farley EV Jr, Napp JM (2013) Climate-related changes in the nutritional condition of young-of-the-year walleye pollock (*Theragra chalcogramma*) from the eastern Bering Sea. Deep Sea Res II 94:150–156

Hertz E, Trudel M, Brodeur RD, Daly EA and others (2015) Continental-scale variability in the feeding ecology of juvenile Chinook salmon along the coastal Northeast Pacific Ocean. Mar Ecol Prog Ser 537:247–263

Hertz E, Trudel M, Tucker S, Beacham TD, Parken C, Mackas D, Mazumder A (2016) Influences of ocean conditions and feeding ecology on the survival of juvenile Chinook salmon (*Oncorhynchus tshawytscha*). Fish Oceanogr 25:407–419

Hunt GL Jr, Coyle KO, Eisner LB, Farley EV and others (2011) Climate impacts on eastern Bering Sea foodwebs: a synthesis of new data and an assessment of the Oscillating Control Hypothesis. ICES J Mar Sci 68:1230–1243

Jennings S, Warr KJ (2003) Environmental correlates of large-scale spatial variation in the $\delta^{15}N$ of marine animals. Mar Biol 142:1131–1140

JGOFS (Joint Global Ocean Flux Study) (1994) Protocols for the Joint Global Ocean Flux Study (JGOFS) Core Measurements. IOC, Scientific Committee on Oceanic Research. Manuals and Guides 29. UNESCO Publishing, Paris

Kline TC Jr (2010) Stable carbon and nitrogen isotope variation in the northern lampfish and *Neocalanus*, marine survival rates of pink salmon, and meso-scale eddies in the Gulf of Alaska. Prog Oceanogr 87:49–60

Kling GW, Fry B, O'Brien WJ (1992) Stable isotopes and planktonic trophic structure in Arctic lakes. Ecology 73: 561–566

Laws EA, Popp BN, Bidigare RR, Kennicutt MC, Macko SA (1995) Dependence of phytoplankton carbon isotopic composition on growth rate and $[CO2]_{aq}$: theoretical considerations and experimental results. Geochim Cosmochim Acta 59:1131–1138

Laws EA, Bidigare RR, Popp BN (1997) Effect of growth rate and CO_2 concentration on carbon isotopic fractionation by the marine diatom *Phaeodactylum tricornutum.* Limnol Oceanogr 42:1552–1560

Legendre P, Legendre LF (1998) Numerical ecology (Vol 24). Elsevier, Amsterdam

Mackas DL, Batten S, Trudel M (2007) Effects on zooplankton of a warmer ocean: recent evidence from the Northeast Pacific. Prog Oceanogr 75:223–252

MacKenzie KM, Longmore C, Preece C, Lucas CH, Trueman CN (2014) Testing the long-term stability of marine isoscapes in shelf seas using jellyfish tissues. Biogeochem 121:441–454

Magozzi S, Yool A, Vander Zanden HB, Wunder MB, Trueman CN (2017) Using ocean models to predict spatial and temporal variation in marine carbon isotopes. Ecosphere 8:e01763

Marsh JM, Mueter FJ, Iken K, Danielson S (2017) Ontogenetic, spatial and temporal variation in trophic level and diet of Chukchi Sea fishes. Deep Sea Res II 135:78–94

McCutchan JH Jr, Lewis WM Jr, Kendall C, McGrath CC (2003) Variation in trophic shift for stable isotope ratios of carbon, nitrogen, and sulfur. Oikos 102:378–390

McMahon KW, Hamady LL, Thorrold SR (2013) A review of ecogeochemistry approaches to estimating movements of marine animals. Limnol Oceanogr 58:697–714

Miller TW, Brodeur RD, Rau GH (2008) Carbon stable isotopes reveal relative contribution of shelf-slope production to the northern California Current pelagic community. Limnol Oceanogr 53:1493–1503

Mills KE, Pershing AJ, Sheehan TF, Mountain D (2013) Climate and ecosystem linkages explain widespread declines in North American Atlantic salmon populations. Glob Change Biol 19:3046–3061

Mullin MM, Rau GH, Eppley RW (1984) Stable nitrogen isotopes in zooplankton: some geographic and temporal variations in the North Pacific. Limnol Oceanogr 29: 1267–1273

Oczkowski A, Markham E, Hanson A, Wigand C (2014) Carbon stable isotopes as indicators of coastal eutrophication. Ecol Appl 24:457–466

Oksanen J, Blanchet FG, Friendly M, Kindt R and others (2018) vegan: community ecology package. R package version 2.4-1. https://CRAN.R-project.org/package=vegan

Parsons TR, Maita Y, Lalli CM (1984) A manual of chemical and biological methods for seawater analysis. Pergamon Press, Oxford

Pinheiro J, Bates D, DebRoy S, Sarkar D, R Core Team (2017) nlme: linear and nonlinear mixed effects models. R package version 3.1-129. https://cran.r-project.org/web/packages/nlme/index.html

Popp BN, Laws EA, Bidigare RR, Dore JE, Hanson KL, Wakeham SG (1998) Effect of phytoplankton cell geometry on carbon isotopic fractionation. Geochim Cosmochim Acta 62:69–77

Popp BN, Graham BS, Olson RJ, Hannides C and others (2007) Insight into the trophic ecology of yellowfin tuna, Thunnus albacares, from compound-specific nitrogen isotope analysis of proteinaceous amino acids. Terr Ecol 1:173–190

Post DM (2002) Using stable isotopes to estimate trophic position: models, methods, and assumptions. Ecology 83: 703–718

Rau GH, Takahashi T, Des Marais DJ (1989) Latitudinal variations in plankton C: implications for CO and productivity in past oceans. Nature 341:516–518

Schell DM (2000) Declining carrying capacity in the Bering Sea: isotopic evidence from whale baleen. Limnol Oceanogr 45:459–462

Schell DM, Barnett BA, Vinette KA (1998) Carbon and nitrogen isotope ratios in zooplankton of the Bering, Chukchi and Beaufort seas. Mar Ecol Prog Ser 162:11–23

Schmittner A, Somes CJ (2016) Complementary constraints from carbon (^{13}C) and nitrogen (^{15}N) isotopes on the glacial ocean's soft-tissue biological pump. Paleoceanography 31:669–693

Schmittner A, Gruber N, Mix AC, Key RM, Tagliabue A, Westberry TK (2013) Biology and air–sea gas exchange controls on the distribution of carbon isotope ratios ($\delta^{13}C$) in the ocean. Biogeosciences 10:5793–5816

Somes CJ, Schmittner A, Galbraith ED, Lehmann MF and others (2010) Simulating the global distribution of nitrogen isotopes in the ocean. Global Biogeochem Cycles 24:GB4019

Spero HJ, Bijma J, Lea DW, Bemis BE (1997) Effect of seawater carbonate concentration on foraminiferal carbon and oxygen isotopes. Nature 390:497–500

Trites AW, Donnelly CP (2003) The decline of Steller sea lions *Eumetopias jubatus* in Alaska: a review of the nutritional stress hypothesis. Mammal Rev 33:3–28

Ware DM, Thomson RE (2005) Bottom-up ecosystem trophic dynamics determine fish production in the Northeast Pacific. Science 308:1280–1284

Warry FY, Reich P, Cook PLM, Mac Nally R, Thomson JR, Woodland RJ (2016) Nitrogen loads influence trophic organization of estuarine fish assemblages. Funct Ecol 30:1723–1733

Weiss RF (1974) Carbon dioxide in water and seawater: the solubility of a non-ideal gas. Mar Chem 2:203–215

Woodland RJ, Rodríguez MA, Magnan P, Glémet H, Cabana G (2012) Incorporating temporally dynamic baselines in isotopic mixing models. Ecology 93:131–144

Zador S (2015) Ecosystem considerations 2014, stock assessment and fishery evaluation report. North Pacific Fisheries Management Council, Anchorage, AK

Editorial responsibility: Antonio Bode, A Coruña, Spain

Submitted: June 8, 2017; Accepted: May 23, 2018
Proofs received from author(s): July 27, 2018